

Probing photonic content of the proton using photon-induced dilepton production in $p + \text{Pb}$ collisions at the LHC

M. Dyndal and A. Glazov

DESY

M. Luszczak and R. Sadykov

Abstract

We propose a new experimental method to validate photon parton distribution function (PDF) inside the proton at LHC energies. It is based on the measurement of dilepton production from the $\gamma p \rightarrow \ell^+ \ell^- + X$ reaction in proton–lead collisions. These experimental conditions guarantee relatively clean environment, both in terms of reconstruction of the final state and in terms of possible background. We firstly calculate the cross sections for this process with collinear photon PDFs, where we identify correct choice of the scale, in analogy to deep inelastic scattering kinematics. We then include the virtuality of probed photon in the calculations, based on modern parameterizations of deep inelastic structure functions. Finally, we find that significant rates of this process are accessible by LHC experiments with existing datasets.

I. INTRODUCTION

Precise calculations of various electroweak reactions in pp collisions at the LHC need to account for, on top of the higher-order corrections, the effects of photon-induced subprocesses. The relevant examples are the production of lepton pairs [1–5] or pairs of electroweak bosons [6–13].

Recently, a precise photon distribution inside the proton has been evaluated in Ref. [14]. This approach provides a model-independent determination of the photon PDF (embedded in so-called LUXqed distribution) and it is based on proton structure function and elastic form factor fits in electron–proton scattering.

Up to date, there are no experimentally clean processes identified that would allow to either strongly constrain or verify the calculations. For example, the extraction of photon PDF from isolated photon production in deep inelastic scattering (DIS) [15] or from inclusive $pp \rightarrow \ell^+ \ell^- + X$ reaction [2, 16, 17] is limited due to large QCD background. On contrary, the elastic part of the photon PDF is verified via exclusive $\gamma\gamma \rightarrow \ell^+ \ell^-$ process, measured in pp collisions by ATLAS [18, 19], CMS [20, 21] and recently by CMS+TOTEM [22] collaborations.

We therefore propose a new experimental method to constrain photonic content of the proton. Thanks to the large fluxes of quasi-real photons from the Pb ion at the LHC, the photon-induced dilepton production in $p + \text{Pb}$ collision configuration is a very clean way to probe photon PDF. This process is shown schematically in Fig. 1, where by analogy to DIS, two leading-order diagrams can be identified. Since the photon flux from the ion scales with Z^2 and QCD-induced cross-sections scale approximately with A , the amount of QCD background is greatly reduced comparing to pp case.

Moreover, as this process does not involve the exchange of color with the photon-emitting nucleus, no significant particle production is expected in the rapidity region between the dilepton system and the nucleus. The photon-emitting nucleus is also expected to produce no neutrons because the photons couple to the entire nucleus. Thus, a combination of a rapidity gap and zero neutrons in the same direction provide straightforward criteria to identify these events experimentally.

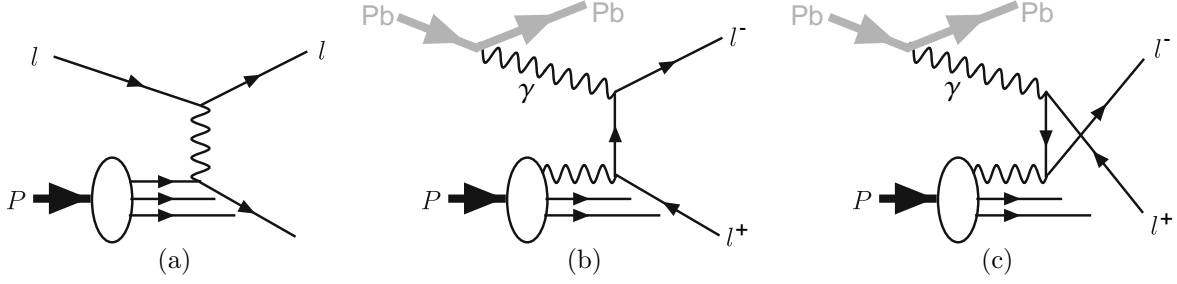


FIG. 1: Schematic graphs for deep inelastic scattering, $\ell^\pm p \rightarrow \ell^\pm + X$ (a) and photon-induced dilepton production, $\gamma p \rightarrow \ell^+ \ell^- + X$, in $p + \text{Pb}$ collisions for t -channel (b) and u -channel (c) lepton exchange.

II. FORMALISM

A. Elastic vertices

In this work we are only interested in the elastic vertices on the nucleus side.

We recall, that for the proton, we can express the photon flux through the electric and magnetic form factors $G_E(Q^2)$ and $G_M(Q^2)$ of the proton:

$$W_T^{\text{el}}(M_X^2, Q^2) = \delta(M_X^2 - m_p^2) Q^2 G_M^2(Q^2), \quad W_L^{\text{el}}(M_X^2, Q^2) = \delta(M_X^2 - m_p^2) 4m_p^2 G_E^2(Q^2). \quad (1)$$

The contribution to the photon flux is then again obtained by contracting

$$\frac{p^\mu p^\nu}{s^2} W_{\mu\nu}^{\text{el}}(M_X^2, Q^2) = \delta(M_X^2 - m_p^2) \left[\left(1 - \frac{z}{2}\right)^2 \frac{4m_p^2 G_E^2(Q^2) + Q^2 G_M^2(Q^2)}{4m_p^2 + Q^2} + \frac{z^2}{4} G_M^2(Q^2) \right] \quad (2)$$

For the nucleus, we follow [23], and replace

$$\frac{4m_p^2 G_E^2(Q^2) + Q^2 G_M^2(Q^2)}{4m_p^2 + Q^2} \longrightarrow Z^2 F_{\text{em}}^2(Q^2). \quad (3)$$

We neglect the magnetic form factor in the following. (It even rigorously vanishes for spinless nuclei.)

For the ^{208}Pb nucleus, we use the realistic formfactor from the STARLIGHT MC.

$$F_{\text{em}}(Q^2) = \frac{3}{(QR_A)^3} \left\{ \sin(QR_A) - QR_A \cos(QR_A) \right\} \frac{1}{1 + a^2 Q^2}. \quad (4)$$

Here

$$R_A = 1.1 A^{1/3} \text{ fm}, \quad a = 0.7 \text{ fm}, \quad Q = \sqrt{Q^2}. \quad (5)$$

Variable	Requirement
lepton transverse momentum, p_T^ℓ	$> 4 \text{ GeV}$
lepton pseudorapidity, $ \eta^\ell $	< 2.4
dilepton invariant mass, $m_{\ell^+\ell^-}$	$> 10 \text{ GeV}$

TABLE I: Definition of the fiducial region used in the studies.

Therefore we obtain the elastic flux

$$\mathcal{F}_{\gamma^* \leftarrow A}^{\text{el}}(z, \mathbf{q}) = \frac{Z^2 \alpha_{\text{em}}}{\pi} (1 - z) \left(\frac{\mathbf{q}^2}{\mathbf{q}^2 + z(M_X^2 - m_A^2) + z^2 m_A^2} \right)^2 F_{\text{em}}^2(Q^2). \quad (6)$$

For ^{208}Pb the charge is $Z = 82$.

III. EXAMPLE EXPERIMENTAL CONFIGURATION AND POSSIBLE BACKGROUND SOURCES

We assume collision setup from recent $p + \text{Pb}$ run at the LHC, carried out at the centre-of-mass energy per nucleon pair $\sqrt{s_{NN}} = 8.16 \text{ TeV}$. Since the energy per nucleon in the proton beam is larger than in the lead beam, the nucleon–nucleon centre-of-mass system has a rapidity in the laboratory frame of $+0.465$.

As an example of method’s applicability, we will use the geometry of ATLAS [24] and CMS [25] detectors in the following. We also consider dimuon-channel only, however the integrated results for ee and $\mu\mu$ channels can be obtained by simply multiplying all cross-sections by a factor of two.

We start with applying minimum transverse momentum requirement of 4 GeV to both muons. This requirement is imposed to ensure high lepton reconstruction and triggering efficiency. Moreover, due to limited acceptance of the detectors, each muon is required to have a pseudorapidity (η^ℓ) that satisfies $|\eta^\ell| < 2.4$ condition. Our calculations are carried out for a minimum dilepton invariant mass $m_{\ell^+\ell^-} = 10 \text{ GeV}$. Such a choice is due to removal of possible contamination from $\Upsilon(\rightarrow \ell^+\ell^-)$ photoproduction process. Summary of all selection requirements is presented in Table I

Possible background for this process can arise from inclusive lepton-pair production, e.g.

from Drell–Yan process [26–29]. These processes would lead to disintegration of the incoming ion, and zero-degree calorimeters (ZDC) [30, 31] can be used to veto very-forward-going neutral fragments which would allow to fully reduce this background. Another background can arise from diffractive interactions, hence possibly mimicking signal topology. However, since the nucleus is a fragile object (with the nucleon binding energy of just 8 MeV) even the softest diffractive interaction will likely result in the emission of a few nucleons from the ion, detectable in the ZDC.

Another background category is the photon-induced process with resolved photon, i.e. $\gamma p \rightarrow Z/\gamma^* + X$ reaction. Here, the rapidity gap is expected to be smaller than in the signal process due to the additional particle production associated with the "photon remnant". Any other residual contamination of this process can be controlled using dedicated region, with a dilepton invariant mass around the Z -boson mass.

IV. RESULTS WITH COLLINEAR PHOTON-PDFS

We start with the calculation of the elastic contribution, $p + \text{Pb} \rightarrow p + \text{Pb} + \ell^+ \ell^-$. In this case the photon flux becomes:

$$f_\gamma^p(x, \mu) = f_\gamma^p(x) \quad (7)$$

and the following parameterization is used []:

$$f_\gamma^p(x) = \frac{\alpha}{\pi} \left(\frac{1 - x + 0.5x^2}{x} \right) \left(\frac{A + 3}{A - 1} \log A - \frac{17}{6} - \frac{4}{3A} + \frac{1}{6A^2} \right), \quad (8)$$

where $A = 1 + \frac{Q_0^2(1-x)}{xm_p^2}$ and $Q_0^2 = 0.71 \text{ GeV}^2$.

The results for the elastic case are cross-checked with the calculation from STARlight MC and a good agreement is found: $\sigma_{fid}^{\text{el}} = 17.5 \text{ nb}$, whereas $\sigma_{fid}^{\text{STARlight}} = 17.0 \text{ nb}$. Both calculations are also corrected by a factor $S^2 = 0.96$ which takes into account the requirement that there be no hadronic interactions between the proton and the ion. This is calculated using STARlight, where the hard-sphere proton–nucleus requirement [32] is used.

Next, for the inelastic case ($\gamma p \rightarrow \ell^+ \ell^- + X$), several recent parameterizations of the photon parton distributions are studied: CT14qed [15], LUXqed17 [33] and NNPDF3.1luxQED [34]. Comparison of several lepton kinematic distributions between different photon-PDFs are shown in Fig. 2,3,4,5.

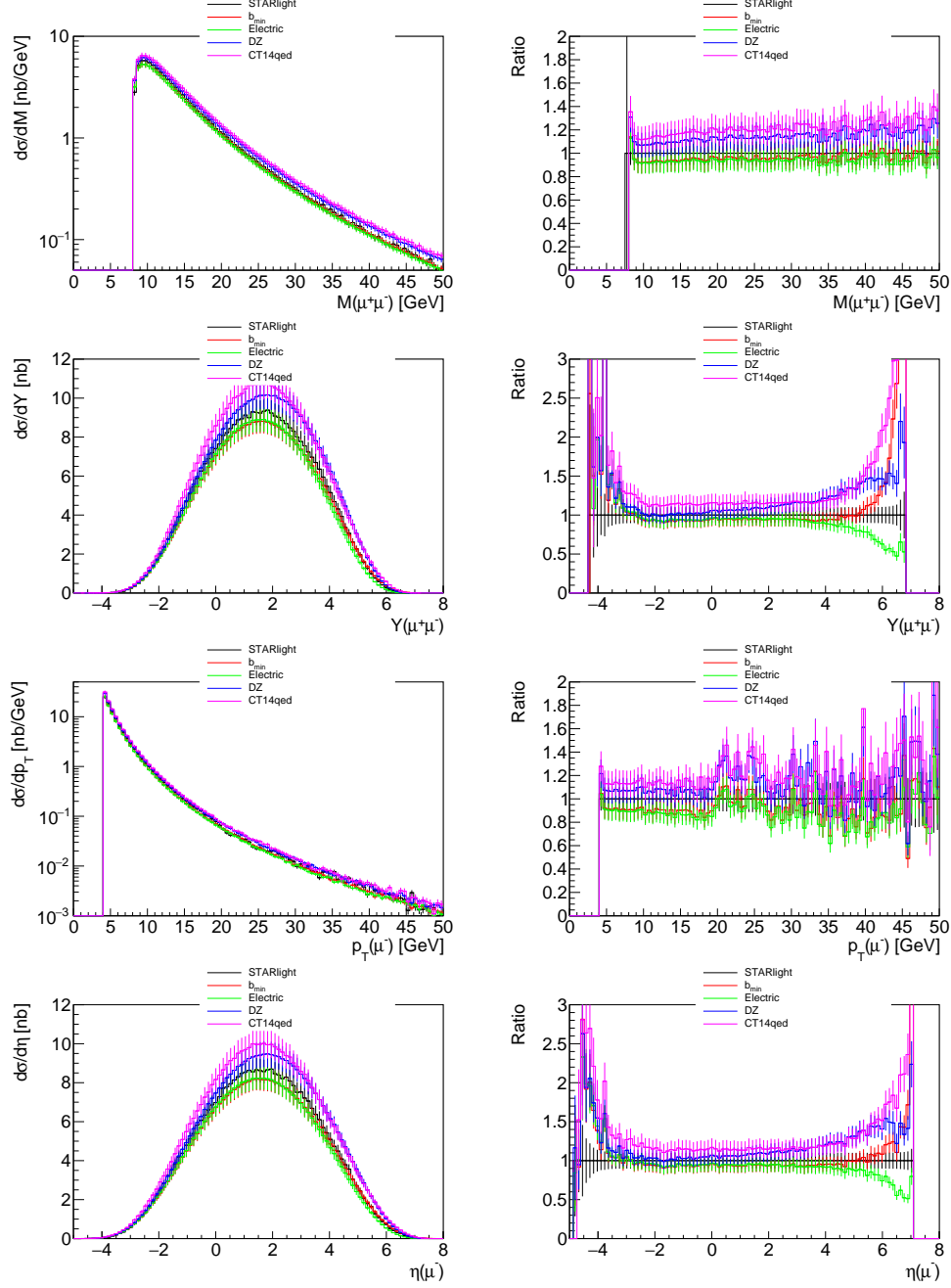


FIG. 2: Elastic distributions (the only cut is on leptons p_T)

The integrated fiducial cross-sections are summarized in Tab. II.

(some discussion here...)

It should be made clear, that the calculations with collinear photons (at lowest order) produce leptons that are back-to-back in transverse kinematics. Therefore, to take the effect of inelastic photon virtuality into account, a dedicated parton shower algorithm should be

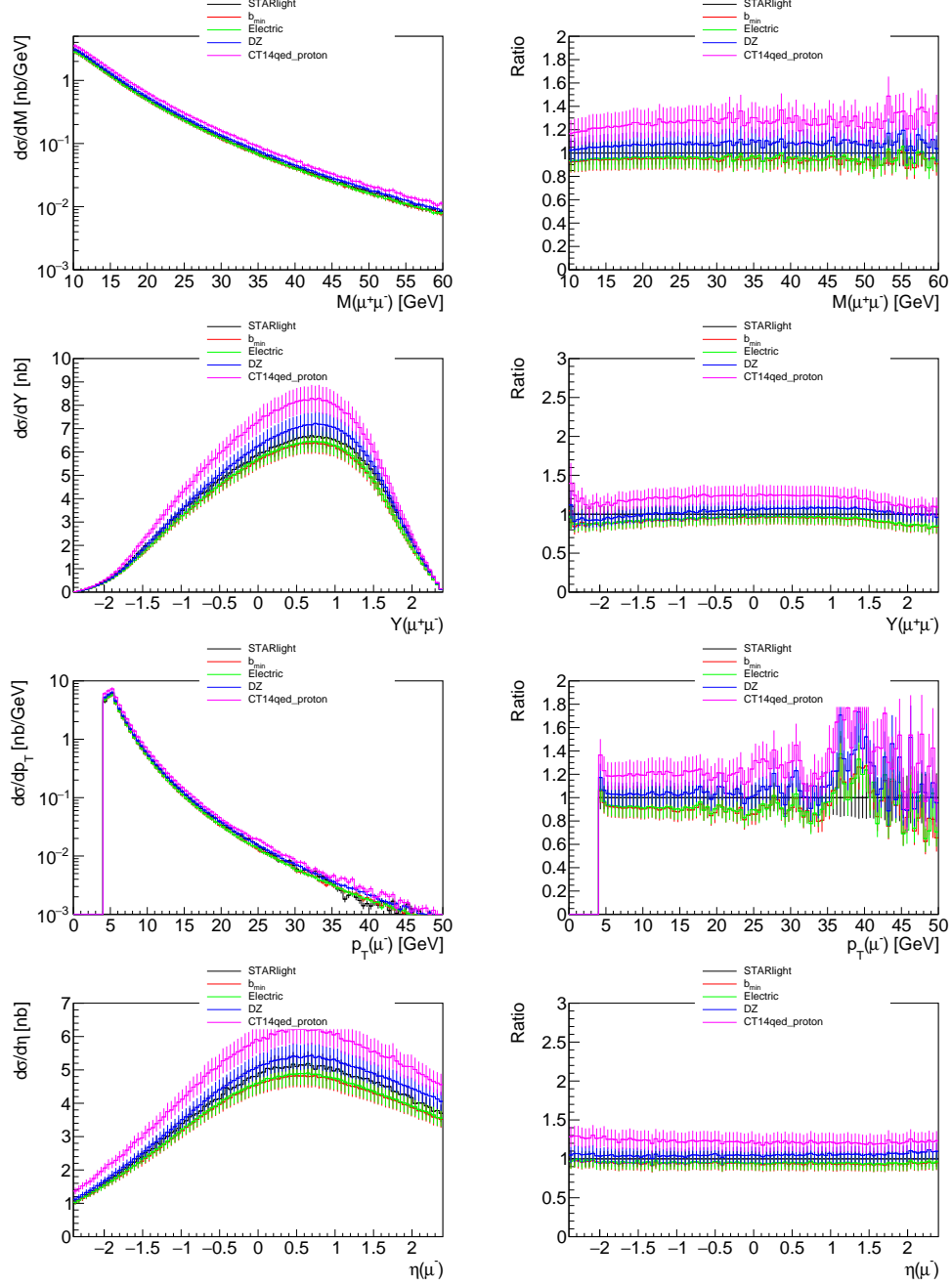


FIG. 3: Elastic distributions (fiducial region)

used.

(mention we don't want to do extra PS; we would rather stick to kt factorization)

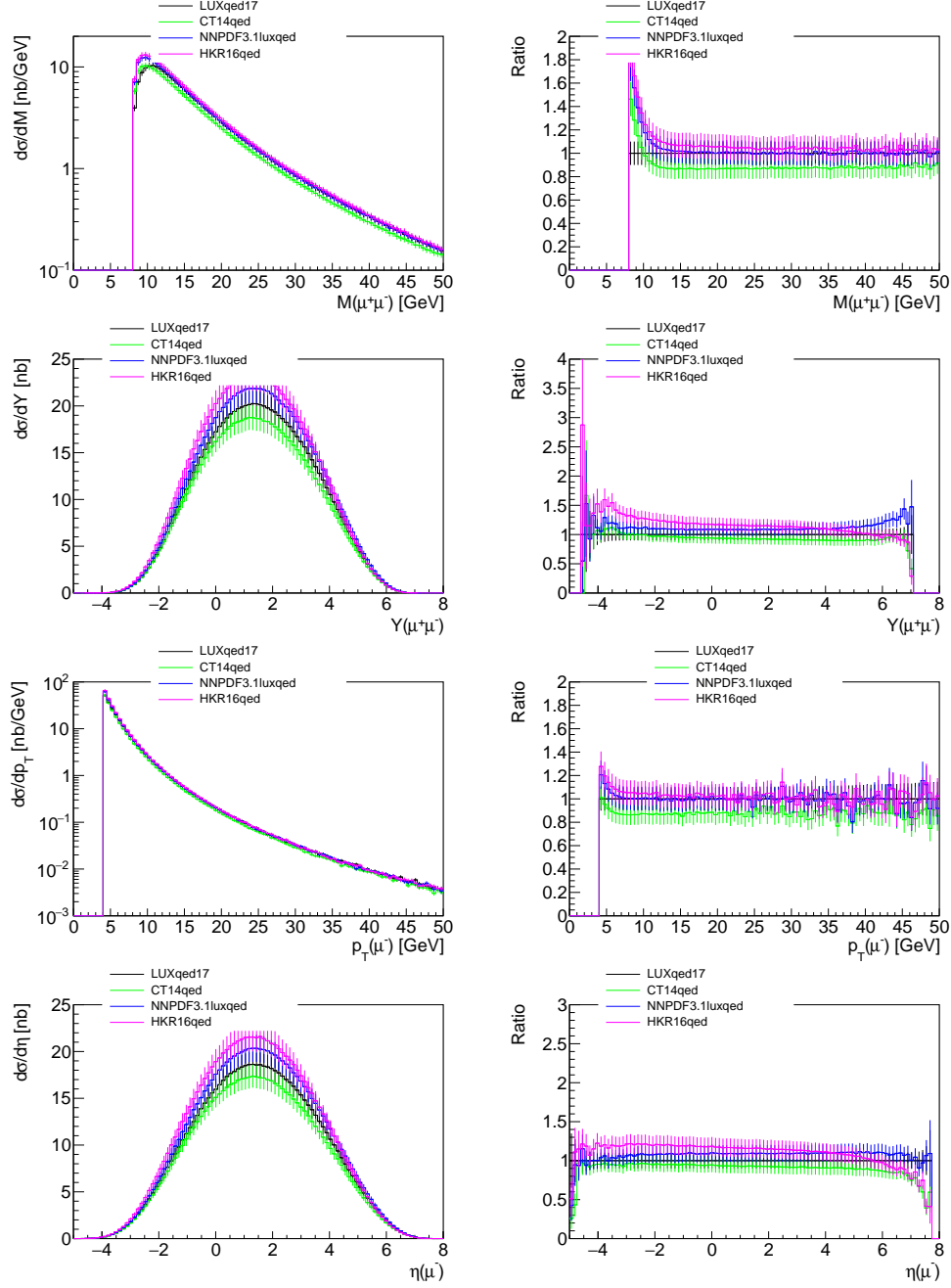


FIG. 4: Inclusive distributions (the only cut is on leptons p_T)

V. RESULTS INCLUDING PHOTON TRANSVERSE MOMENTUM

VI. DISCUSSION

We take the opportunity to calculate expected number of events for realistic assumption on total integrated luminosity. based on the previous $p\text{Pb}$ runs at the LHC, we assume

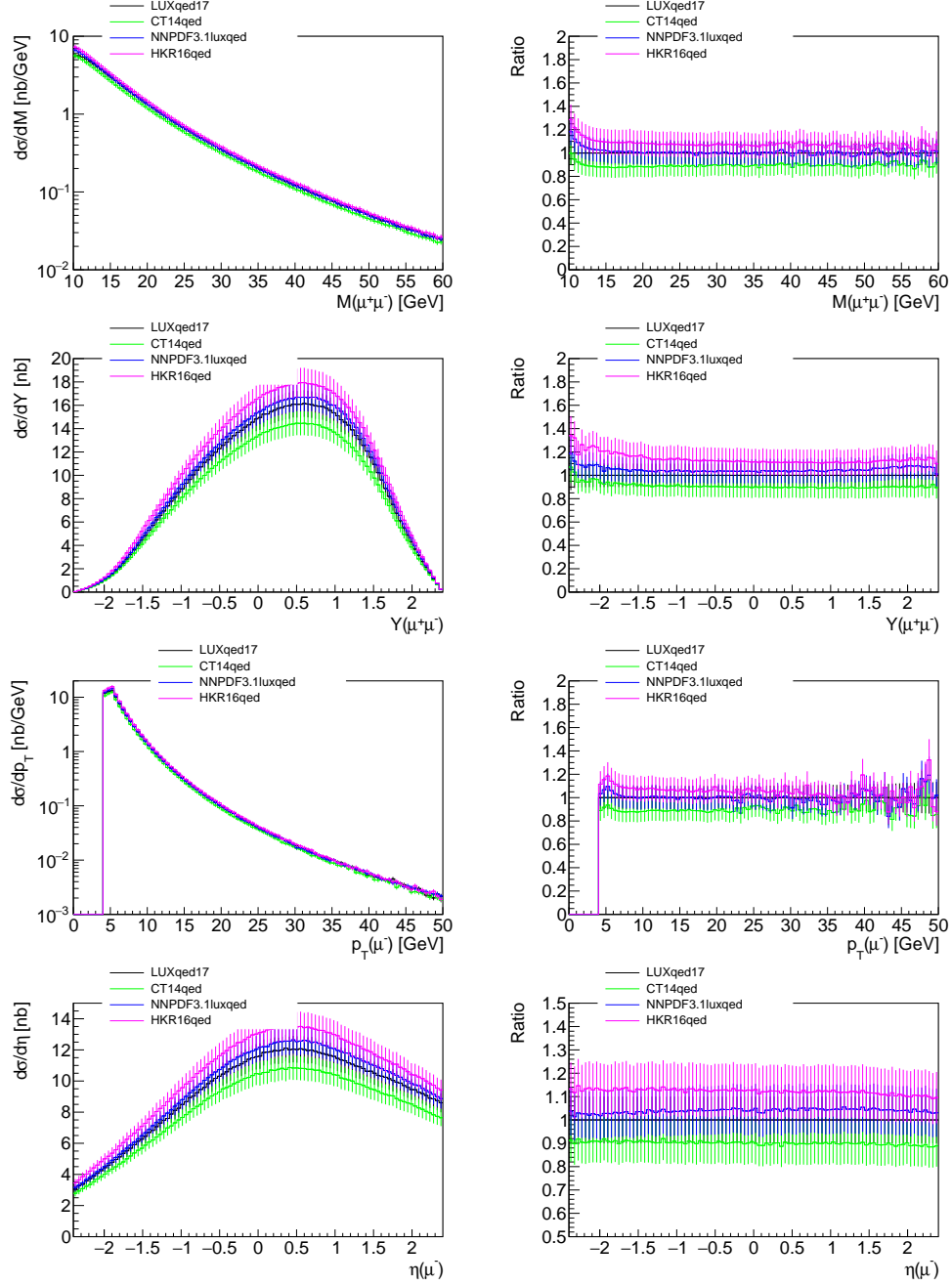


FIG. 5: Inclusive distributions (fiducial region)

$$\int L dt = 200 \text{ nb}^{-1}.$$

(show some table(s) here)

Contribution	$p_T(\ell) > 4 \text{ GeV}$	$p_T(\ell) > 4 \text{ GeV}, \eta(\ell) < 2.4,$ $M(\ell^+\ell^-) > 10 \text{ GeV}$
$\gamma_{el}\gamma_{el} [b_{min} = 0.7 fm]$	45.5(2) nb	17.3(1) nb
$\gamma_{el}\gamma_{el} [\text{Electric}]$	44.9(1) nb	17.5(1) nb
$\gamma_{el}\gamma_{el} [\text{DZ}]$	53.3(1) nb	19.4(1) nb
$\gamma_{el}\gamma_{el} [\text{CT14qed}]$	48.4(1) nb	17.6(1) nb
$\gamma_{inc}\gamma_{el} [\text{CT14qed}]$	98.0(1) nb	39.7(1) nb
$\gamma_{inc}\gamma_{el} [\text{LUXqed17}]$	105.8(1) nb	44.1(1) nb
$\gamma_{inc}\gamma_{el} [\text{NNPDF3.1luxqed}]$	115.6(1) nb	45.9(1) nb
$\gamma_{inc}\gamma_{el} [\text{HKR16qed}]$	121.6(1) nb	49.4(1) nb

TABLE II: Cross sections for different contributions

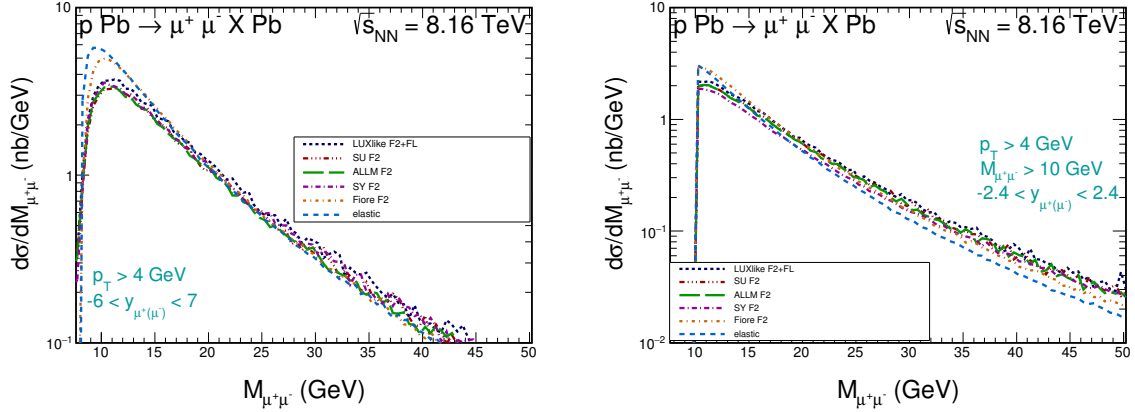


FIG. 6: The elastic - elastic and the inelastic-elastic contribution to dilepton invariant mass distributions for different structure functions. In the left panel we show the results for the whole phase space, while in the right panel only for the fiducial region.

VII. SUMMARY

In summary, we propose a method that would unambiguously allow to test and constrain the photon parton distribution at LHC energies.

contribution	$\sqrt{s_{NN}} = 8.16 \text{ TeV}$	$\sqrt{s_{NN}} = 8.16 \text{ TeV}$
	without cuts	$p_T > 4 \text{ GeV}, y < 2.4, M_{l+l-} > 10 \text{ GeV}$
LUX-like F2+FL $\gamma_{in}\gamma_{el}$	42.57	17.07
LUX-like F2 $\gamma_{in}\gamma_{el}$	43.58	17.44
ALLM97 F2 $\gamma_{in}\gamma_{el}$	41.72	16.43
Fiore et al. (parametrization of JLAB data) $\gamma_{in}\gamma_{el}$	45.24	18.36
SU F2 $\gamma_{in}\gamma_{el}$	41.72	16.70
SY F2 $\gamma_{in}\gamma_{el}$	40.38	15.99
Elastic- Elastic $\gamma_{el}\gamma_{el}$	47.89	18.26

TABLE III: Cross sections (in nb) for different contributions and different structure functions: LUX-like, ALLM97, Fiore, SU and SY. (the cross section was scaled by factors: 0.96 (elastic-elastic); 0.95 (elastic-inelastic) for proton-ion absorption (multiple interactions))

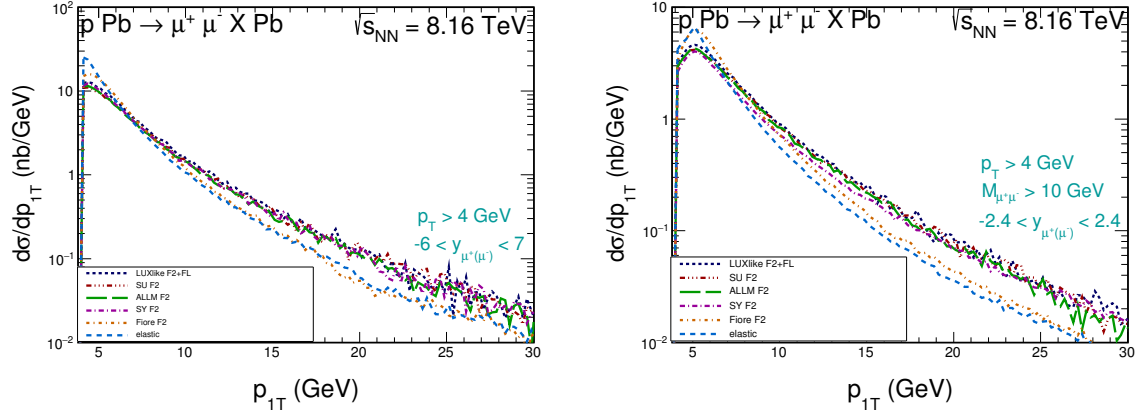


FIG. 7: Transverse momentum distribution of μ^+ or μ^- for elastic - elastic and inelastic - elastic different structure functions: LUX-like, ALLM97, Fiore et al., SU and SY (in the left panel we show the results for the whole phase space, while in the right panel only for the fiducial region).

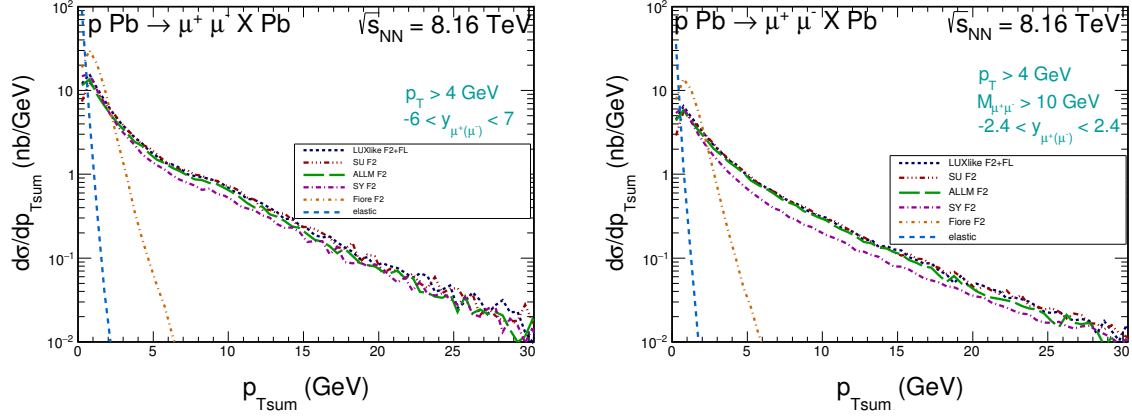


FIG. 8: Distribution in transverse momentum of the $\mu^+\mu^-$ pairs for elastic - elastic and inelastic-elastic contributions for different structure functions: LUX-like, ALLM97, Fiore at all., SU and SY. (in the left panel we show the results for the whole phase space, while in the right panel only for the fiducial region).

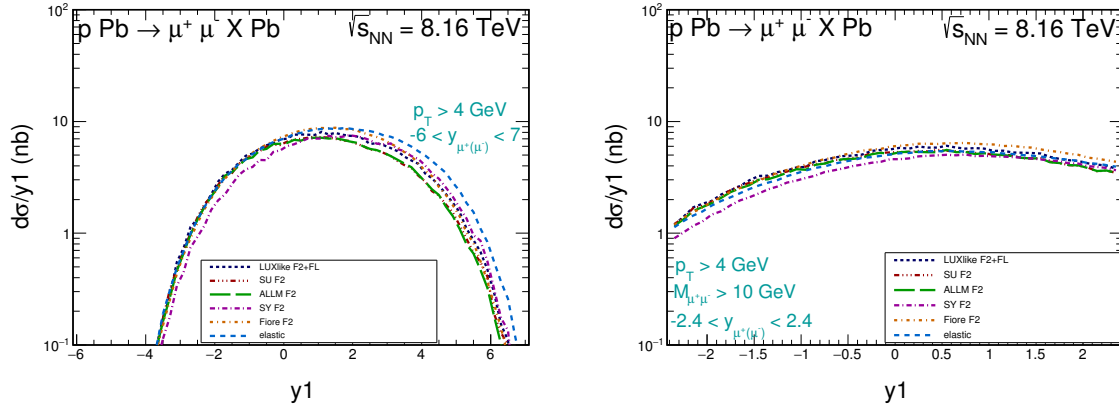


FIG. 9: Rapidity distribution of μ^+ or μ^- leptons for elastic - elastic and inelastic-elastic contributions for different structure functions: LUX-like, ALLM97, Fiore at all., SU and SY. (in the left panel we show the results for the whole phase space, while in the right panel only for the fiducial region).

References

-
- [1] ATLAS Collaboration, G. Aad et al., *Measurement of the low-mass Drell-Yan differential cross section at $\sqrt{s} = 7$ TeV using the ATLAS detector*, JHEP **06** (2014) 112,

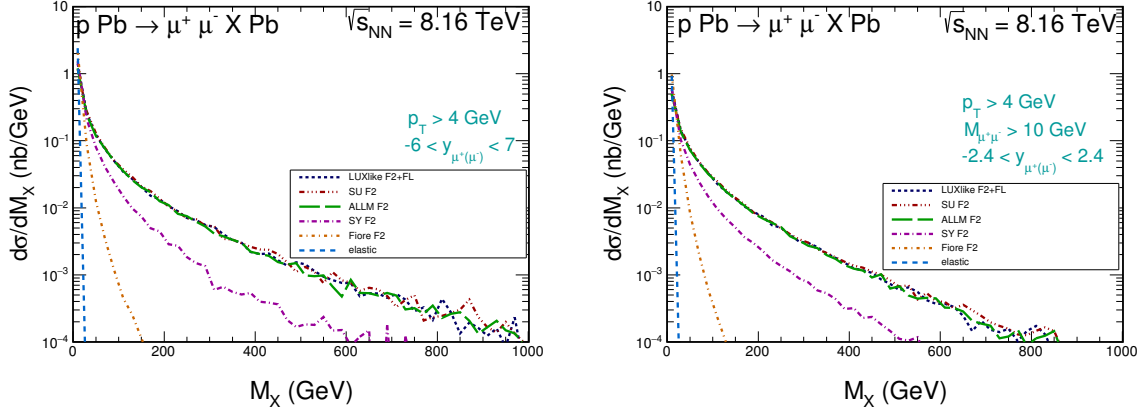


FIG. 10: Missing mass distributions for elastic-elastic photon-photon contributions and elastic-inelastic photon-photon contributions for different structure functions: LUX-like, ALLM97, Fiore at all., SU and SY. (in the left panel we show the results for the whole phase space, while in the right panel only for the fiducial region).

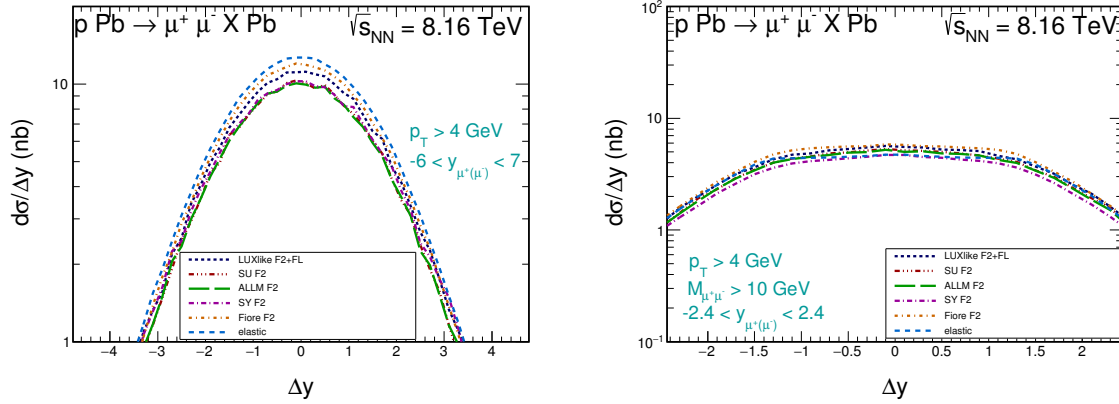


FIG. 11: Distribution in rapidity distance between $\mu^+\mu^-$ leptons. The calculation for the $\gamma - \gamma$ contribution was performed for different structure functions. The left panel shows results without cuts while the right panel shows results with ATLAS cuts.

arXiv:1404.1212 [hep-ex].

- [2] ATLAS Collaboration, G. Aad et al., *Measurement of the double-differential high-mass Drell-Yan cross section in pp collisions at $\sqrt{s} = 8$ TeV with the ATLAS detector*, JHEP **08** (2016) 009, arXiv:1606.01736 [hep-ex].

- [3] E. Accomando, J. Fiaschi, F. Hautmann, S. Moretti, and C. H. Shepherd-Themistocleous, *Photon-initiated production of a dilepton final state at the LHC: Cross section versus*

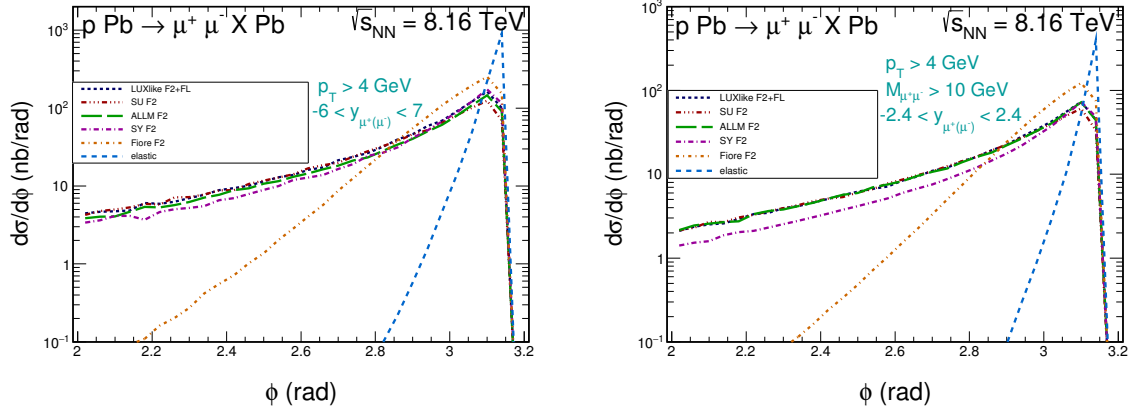


FIG. 12: Distributions for azimuthal angle between $\mu^+\mu^-$ leptons. (in the left panel we show the results for the whole phase space, while in the right panel only for the fiducial region).

- forward-backward asymmetry studies*, Phys. Rev. **D95** (2017) no. 3, 035014, [arXiv:1606.06646 \[hep-ph\]](#).
- [4] M. Luszczak, W. Schafer, and A. Szczurek, *Two-photon dilepton production in proton-proton collisions: two alternative approaches*, Phys. Rev. **D93** (2016) no. 7, 074018, [arXiv:1510.00294 \[hep-ph\]](#).
- [5] L. A. Harland-Lang, V. A. Khoze, and M. G. Ryskin, *The photon PDF in events with rapidity gaps*, Eur. Phys. J. **C76** (2016) no. 5, 255, [arXiv:1601.03772 \[hep-ph\]](#).
- [6] M. Luszczak, A. Szczurek, and C. Royon, *W^+W^- pair production in proton-proton collisions: small missing terms*, JHEP **02** (2015) 098, [arXiv:1409.1803 \[hep-ph\]](#).
- [7] A. Denner, S. Dittmaier, M. Hecht, and C. Pasold, *NLO QCD and electroweak corrections to $Z + \gamma$ production with leptonic Z-boson decays*, JHEP **02** (2016) 057, [arXiv:1510.08742 \[hep-ph\]](#).
- [8] M. Dyndal and L. Schoeffel, *Four-lepton production from photon-induced reactions in pp collisions at the LHC*, Acta Phys. Polon. **B47** (2016) 1645, [arXiv:1511.02065 \[hep-ph\]](#).
- [9] M. Ababekri, S. Dulat, J. Isaacson, C. Schmidt, and C. P. Yuan, *Implication of CMS data on photon PDFs*, [arXiv:1603.04874 \[hep-ph\]](#).
- [10] B. Biedermann, M. Billoni, A. Denner, S. Dittmaier, L. Hofer, B. Jger, and L. Salfelder, *Next-to-leading-order electroweak corrections to $pp \rightarrow W^+W^- \rightarrow 4$ leptons at the LHC*, JHEP **06** (2016) 065, [arXiv:1605.03419 \[hep-ph\]](#).
- [11] B. Biedermann, A. Denner, S. Dittmaier, L. Hofer, and B. Jger, *Electroweak corrections to*

- $pp \rightarrow \mu^+ \mu^- e^+ e^- + X$ at the LHC: a Higgs background study, Phys. Rev. Lett. **116** (2016) no. 16, 161803, [arXiv:1601.07787 \[hep-ph\]](#).
- [12] Y. Wang, R.-Y. Zhang, W.-G. Ma, X.-Z. Li, and L. Guo, *QCD and electroweak corrections to ZZ +jet production with Z -boson leptonic decays at the LHC*, Phys. Rev. **D94** (2016) no. 1, 013011, [arXiv:1604.04080 \[hep-ph\]](#).
- [13] M. Luszczak, W. Schafer, and A. Szczurek, *Production of W^+W^- pairs via $\gamma^*\gamma^* \rightarrow W^+W^-$ subprocess with photon transverse momenta*, JHEP **05** (2018) 064, [arXiv:1802.03244 \[hep-ph\]](#).
- [14] A. Manohar, P. Nason, G. P. Salam, and G. Zanderighi, *How bright is the proton? A precise determination of the photon parton distribution function*, Phys. Rev. Lett. **117** (2016) no. 24, 242002, [arXiv:1607.04266 \[hep-ph\]](#).
- [15] C. Schmidt, J. Pumplin, D. Stump, and C. P. Yuan, *CT14QED parton distribution functions from isolated photon production in deep inelastic scattering*, Phys. Rev. **D93** (2016) no. 11, 114015, [arXiv:1509.02905 \[hep-ph\]](#).
- [16] NNPDF Collaboration, R. D. Ball, V. Bertone, S. Carrazza, L. Del Debbio, S. Forte, A. Guffanti, N. P. Hartland, and J. Rojo, *Parton distributions with QED corrections*, Nucl. Phys. **B877** (2013) 290–320, [arXiv:1308.0598 \[hep-ph\]](#).
- [17] xFitter Developers’ Team Collaboration, F. Giuli et al., *The photon PDF from high-mass Drell-Yan data at the LHC*, Eur. Phys. J. **C77** (2017) no. 6, 400, [arXiv:1701.08553 \[hep-ph\]](#).
- [18] ATLAS Collaboration, G. Aad et al., *Measurement of exclusive $\gamma\gamma \rightarrow \ell^+\ell^-$ production in proton-proton collisions at $\sqrt{s} = 7$ TeV with the ATLAS detector*, Phys. Lett. **B749** (2015) 242–261, [arXiv:1506.07098 \[hep-ex\]](#).
- [19] ATLAS Collaboration, M. Aaboud et al., *Measurement of the exclusive $\gamma\gamma \rightarrow \mu^+\mu^-$ process in proton-proton collisions at $\sqrt{s} = 13$ TeV with the ATLAS detector*, Phys. Lett. **B777** (2018) 303–323, [arXiv:1708.04053 \[hep-ex\]](#).
- [20] CMS Collaboration, S. Chatrchyan et al., *Exclusive photon-photon production of muon pairs in proton-proton collisions at $\sqrt{s} = 7$ TeV*, JHEP **01** (2012) 052, [arXiv:1111.5536 \[hep-ex\]](#).
- [21] CMS Collaboration, S. Chatrchyan et al., *Search for exclusive or semi-exclusive photon pair production and observation of exclusive and semi-exclusive electron pair production in pp*

- collisions at $\sqrt{s} = 7$ TeV*, JHEP **11** (2012) 080, [arXiv:1209.1666 \[hep-ex\]](#).
- [22] CMS, TOTEM Collaboration, A. M. Sirunyan et al., *Observation of proton-tagged, central (semi)exclusive production of high-mass lepton pairs in pp collisions at 13 TeV with the CMS-TOTEM precision proton spectrometer*, Submitted to: JHEP (2018) , [arXiv:1803.04496 \[hep-ex\]](#).
- [23] V. M. Budnev, I. F. Ginzburg, G. V. Meledin, and V. G. Serbo, *The two photon particle production mechanism. Physical problems. Applications. Equivalent photon approximation*, Phys. Rept. **15** (1975) 181.
- [24] ATLAS Collaboration, G. Aad et al., *The ATLAS Experiment at the CERN Large Hadron Collider*, JINST **3** (2008) S08003.
- [25] CMS Collaboration, S. Chatrchyan et al., *The CMS Experiment at the CERN LHC*, JINST **3** (2008) S08004.
- [26] S. D. Drell and T.-M. Yan, *Massive Lepton Pair Production in Hadron-Hadron Collisions at High-Energies*, Phys. Rev. Lett. **25** (1970) 316–320. [Erratum: Phys. Rev. Lett.25,902(1970)].
- [27] ATLAS Collaboration, G. Aad et al., *Z boson production in p+Pb collisions at $\sqrt{s_{NN}} = 5.02$ TeV measured with the ATLAS detector*, Phys. Rev. **C92** (2015) no. 4, 044915, [arXiv:1507.06232 \[hep-ex\]](#).
- [28] CMS Collaboration, V. Khachatryan et al., *Study of Z boson production in pPb collisions at $\sqrt{s_{NN}} = 5.02$ TeV*, Phys. Lett. **B759** (2016) 36–57, [arXiv:1512.06461 \[hep-ex\]](#).
- [29] ALICE Collaboration, J. Adam et al., *W and Z boson production in p-Pb collisions at $\sqrt{s_{NN}} = 5.02$ TeV*, JHEP **02** (2017) 077, [arXiv:1611.03002 \[nucl-ex\]](#).
- [30] ALICE Collaboration, G. Dellacasa et al., *ALICE technical design report of the zero degree calorimeter (ZDC)*, . CERN-LHCC-99-05.
- [31] ATLAS Collaboration, *Zero degree calorimeters for ATLAS*, . CERN-LHCC-2007-01.
- [32] S. R. Klein, J. Nystrand, J. Seger, Y. Gorbunov, and J. Butterworth, *STARlight: A Monte Carlo simulation program for ultra-peripheral collisions of relativistic ions*, Comput. Phys. Commun. **212** (2017) 258–268, [arXiv:1607.03838 \[hep-ph\]](#).
- [33] A. V. Manohar, P. Nason, G. P. Salam, and G. Zanderighi, *The Photon Content of the Proton*, JHEP **12** (2017) 046, [arXiv:1708.01256 \[hep-ph\]](#).
- [34] NNPDF Collaboration, V. Bertone, S. Carrazza, N. P. Hartland, and J. Rojo, *Illuminating*

the photon content of the proton within a global PDF analysis, [arXiv:1712.07053](#)
[hep-ph].